

## Soret and Dufour Effects on MHD Free Convection Heat and Mass Transfer Flow over a Stretching Vertical Plate with Suction and Heat Source/Sink

M. J. Subhakar<sup>1</sup>, K. Gangadhar<sup>2</sup>

<sup>1</sup> HOD of Mathematics, Noble College, Machilipatnam, A.P. 521001.India.

<sup>2</sup> Assistant Professor, Dept of mathematics, ANUOC, Ongole-523001, A.P, India.

**ABSTRACT:** The present paper is to investigate the combined effect of the free convective heat and mass transfer on the unsteady two-dimensional boundary layer flow over a stretching vertical plate in the presence of heat generation/absorption, and soret and dufour effects. The flow is subject to magnetic field normal to the plate. The governing nonlinear partial differential equations have been reduced to the coupled nonlinear ordinary differential equations by the similarity transformations. The resulting equations are solved numerically by using Runge-Kutta fourth order method along with shooting technique. The velocity and temperature distributions are discussed numerically and presented through graphs. The numerical values of skin-friction coefficient and Nusselt number at the plate are derived, discussed numerically for various values of physical parameters and presented through Tables. The numerical results are benchmarked with the earlier study by Magyari and Keller [24], and Srinivasachari and Ram Reddy [23] and found to be in excellent agreement.

**Keywords:** Free Convection, heat and mass transfer, heat generation/absorption, MHD, Suction, Stretching vertical plate.

### I. INTRODUCTION

The effect of free convection on the accelerated flow of a viscous incompressible fluid past an infinite vertical plate with suction has many important technological applications in the astrophysical, geophysical and engineering problems. The heating of rooms and buildings by the use of radiators is a familiar example of heat transfer by free convection. Heat losses from hot pipes, ovens etc. Heat and mass transfer play an important role in manufacturing industries for the design of fins, steel rolling, nuclear power plants, gas turbines and various propulsion devices for aircraft, combustion and furnace design, materials processing, energy utilization, temperature measurements.

The unsteady heat transfer problems over a stretching surface, which is stretched with a velocity that depends on time, are considered by Andersson et al.[1] who studied the heat transfer over an unsteady stretching surface. Ishak et al.[2] have studied the heat transfer over an unsteady stretching vertical surface. Ishak et al.[3] have also investigated the unsteady laminar boundary layer over a continuously stretching permeable surface. Rajesh [4] has studied radiation effects on MHD free convection flow near a vertical plate with ramped wall temperature. El-Arabawy [5] studied the effect of suction/injection on a micropolar fluid past a continuously moving plate in the presence of radiation. Loganathan[6] studied the effects of thermal conductivity on unsteady MHD free convective flow over a semi infinite vertical plate.

In recent years, considerable attention has been devoted to study the MHD flows and heat transfer because of the applications in engineering, agriculture, petroleum industries, geophysics, and astrophysics. Kinyanjui et al. [7] studied the transient free convection heat over an impulsively started vertical plate in the presence of thermal radiation. Al-Odat and Al-Azab [8] numerically studied the transient MHD free convective

heat and mass transfer over a moving vertical surface in the presence of a homogeneous chemical reaction of first order. Palani and Srikanth [9] studied the MHD flow of an

electrically conducting fluid over a semi-infinite vertical plate under the influence of the transversely applied magnetic field. Makinde[10] investigated the MHD boundary layer flow with the heat and mass transfer over a moving vertical plate in the presence of magnetic field and convective heat exchange at the surface.

The heat source/sink effects in thermal convection are significant where there may exist high temperature differences between the surface (e.g. space craft body) and the ambient fluid. Heat generation is also important in the context of exothermic or endothermic chemical reaction. Tania et al [11] has investigated the Effects of radiation, heat generation and viscous dissipation on MHD free convection flow along a stretching sheet. Furthermore, Moalem [12] studied the effect of temperature dependent heat sources taking place in electrically heating on the heat transfer within a porous medium. Vajravelu and Nayfeh [13] reported on the hydro magnetic convection at a cone and a wedge in the presence of temperature dependent heat generation or absorption effects. Moreover, Chamkha [14] studied the effect of heat generation or absorption on hydro magnetic three-dimensional free convection flow over a vertical stretching surface. Radiation and mass transfer effects on MHD free convection fluid flow embedded in a porous medium with heat generation/absorption was studied by Shankar et al [15]

The Dufour and Soret effects were neglected in many reported research studies, since they are of a smaller order of magnitude than the effects described by Fourier's and Fick's laws. When the heat and mass transfer occurs simultaneously in a moving fluid, the relations between the fluxes and the driving potentials are more complicated. It was found that an energy flux can be generated not only by the temperature gradients but also by the composition gradients. The mass transfer caused by the temperature gradient is called the Soret effect, while the heat transfer caused by the concentration gradient is called the Dufour effect. However, such effects become crucial when the density difference exists in the flow regimes. The Soret effect, for instance, has been utilized for isotope separation.

In a mixture between gases with very light molecular weight (He, H<sub>2</sub>) and medium molecular weight (N<sub>2</sub>, air), the Dufour effect was found to be of considerable magnitude such that it cannot be neglected (Eckert and Drak [16]). The Dufour and Soret effects were studied by many researchers. Kafoussias and Williams [17] studied the thermo-diffusion and diffusion-thermo effects on the mixed free-forced convective and mass transfer of steady laminar boundary layer flow over a vertical flat. Mohamad [18] studied the Soret effect on the unsteady magnetohydrodynamics (MHD) free convection heat and mass transfer flow past a semi-infinite vertical plate in a Darcy porous medium in the presence of chemical reaction and heat generation. Afify[19] carried out a numerical analysis to study the free convective heat and mass transfer of an incompressible electrically conducting fluid over a stretching sheet in the presence of suction and injection with the Soret and Dufour effects. Shyam et al.[20] examined the Soret and Dufour effects on the MHD natural convection over a vertical surface embedded in a Darcy porous medium in the presence of thermal radiation. Numerical investigation of Dufour and Soret effects on unsteady MHD natural convection flow past vertical plate embedded in non-Darcy porous medium was investigated by Al-Odat and Al-Ghamdi [21]. Ali-Chamkha and Mansour[22] examined the effect of chemical reaction, thermal radiation, and heat generation or absorption on the unsteady MHD free convective heat and mass transfer along an infinite vertical plate. Soret and Dufour Effects on Mixed Convection from an Exponentially Stretching Surface was discussed by Srinivasacharya and RamReddy [23]

The object of the present chapter is to analyze the combined effect of the free convective heat and mass transfer on the unsteady two-dimensional boundary layer flow over a stretching vertical plate by taking heat generation/absorption, and soret and dufour effects into account. The governing boundary layer equations have been transformed to a two-point boundary value problem in similarity variables and the resultant problem is solved numerically using the Runge-Kutta method with shooting technique. The effects of various governing parameters on the fluid velocity, temperature, concentration, skin-friction coefficient, Nusselt number and Sherwood number are shown in figures and tables and analyzed in detail.

## II. MATHEMATICAL ANALYSIS

An unsteady two-dimensional laminar boundary layer flow of an incompressible fluid over a stretching vertical plate is considered. The fluid is assumed to be Newtonian, electrically conducting and its property variations due to temperature and chemical species concentration are limited to fluid density. The density variation and the effects of the buoyancy are taken into account in the momentum equation (Boussinesq's approximation). The x-axis is taken along the plate in the upward direction and the y-axis is taken normal to it. A uniform magnetic field is applied in the direction perpendicular to the plate. The transverse applied magnetic field and magnetic Reynolds number are assumed to be very small, so that the induced magnetic field and Hall effects are negligible. Now, under the above assumptions, the governing boundary layer equations of the flow field are:

Continuity equation

$$\frac{\partial u}{\partial x} + \frac{\partial v}{\partial y} = 0 \quad (2.1)$$

Momentum equation

$$\frac{\partial u}{\partial t} + u \frac{\partial u}{\partial x} + v \frac{\partial u}{\partial y} = \nu \frac{\partial^2 u}{\partial y^2} - \frac{\sigma B_0^2}{\rho} u + g \beta_T (T - T_\infty) + g \beta_c (C - C_\infty) \quad (2.2)$$

Energy equation

$$\frac{\partial T}{\partial t} + u \frac{\partial T}{\partial x} + v \frac{\partial T}{\partial y} = \alpha \frac{\partial^2 T}{\partial y^2} + \frac{D_m k_T}{c_s c_p} \frac{\partial^2 C}{\partial y^2} + q(T - T_\infty) \quad (2.3)$$

Species equation

$$\frac{\partial C}{\partial t} + u \frac{\partial C}{\partial x} + v \frac{\partial C}{\partial y} = D_m \frac{\partial^2 C}{\partial y^2} + \frac{D_m k_T}{T_m} \frac{\partial^2 T}{\partial y^2} \quad (2.4)$$

The boundary conditions for the velocity, temperature and concentration fields are

$$u = U, v = V_w, T = T_w, C = C_w \text{ at } y = 0 \\ u \rightarrow 0, T \rightarrow T_\infty, C \rightarrow C_\infty \text{ as } y \rightarrow \infty \text{ for } t > 0 \quad (2.5)$$

where  $u$ ,  $v$ ,  $T$  and  $C$  are the fluid x-component of velocity, y-component of velocity, temperature and concentration respectively,  $\nu$  is the fluid kinematics viscosity,  $\rho$  - the density,  $\sigma$  - the electric conductivity of the fluid,  $\beta_T$  and  $\beta_c$  - the coefficients of thermal and concentration expansions respectively,  $\alpha$  - the thermal conductivity,  $C_\infty$  - the free stream concentration,  $B_0$  - the magnetic induction,  $U$  - the free stream velocity,  $D_m$  - the mass diffusivity and  $g$  is the gravitational acceleration,  $T_w$  is the temperature of the hot fluid at the left surface of the plate,  $C_w$  is the species concentration at the plate surface, The mass concentration equation (2.1) is satisfied by the Cauchy-Riemann equations

$$u = \frac{\partial \psi}{\partial y}, v = -\frac{\partial \psi}{\partial x} \quad (2.6)$$

where  $\psi(x, y)$  is the stream function.

To transform equations (2.2) - (2.4) into a set of ordinary differential equations, the following similarity transformations and dimensionless variables are introduced.

$$\eta = y \sqrt{\frac{c}{\nu(1-\lambda t)}}, \quad \psi = x \sqrt{\frac{c\nu}{1-\lambda t}} f(\eta) \\ T = T_\infty + T_w \left[ \frac{cx}{2\nu(1-\lambda t)^2} \right] \theta(\eta) \\ C = C_\infty + C_w \left[ \frac{cx}{2\nu(1-\lambda t)^2} \right] \phi(\eta) \\ M = \frac{\sigma B_0^2 (1-\lambda t)}{\rho c}, \quad Gr = \frac{g \beta_T T_w}{2c\nu}, \quad Gc = \frac{g \beta_c C_w}{2c\nu}, \\ D_f = \frac{D_m k_T C_w}{\nu c_s c_p T_w}, \quad Sr = \frac{D_m k_T T_w}{\nu T_m C_w}, \quad Q = \frac{cq}{1-\lambda t} \\ Pr = \frac{\nu}{\alpha}, \quad Sc = \frac{\nu}{D_m}, \quad A = \frac{\lambda}{c} \quad (2.7)$$

where  $\eta$  - similarity variable,  $f$  - dimensionless stream function,  $\theta$  - dimensionless temperature,  $\phi$  - dimensionless

concentration,  $M$  - the Magnetic field parameter,  $Gr$  - the thermal Grashof number,  $Gc$  - the solutal Grashof number,  $D_f$  - the Dufour number,  $Sr$  - the Soret number,  $Q$  - the heat generation/absorption parameter,  $Pr$  - the Prandtl number,  $Sc$  - the Schmidt number and  $A$  - Unsteadiness parameter.

In view of equations (2.6) and (2.7), Equations (2.2) to (2.4) transform into

$$f'''(\eta) + f(\eta)f''(\eta) - \frac{A}{2}\eta f'(\eta) + Gr\theta(\eta) + Gc\phi(\eta) - Mf'(\eta) = 0 \quad (2.8)$$

$$\theta''(\eta) + Pr \left[ f(\eta)\theta'(\eta) - \frac{A}{2}\eta\theta'(\eta) - \theta f'(\eta) + Du\phi''(\eta) \right] = 0 \quad (2.9)$$

$$\phi''(\eta) + Sc \left[ f(\eta)\phi'(\eta) - \frac{A}{2}\eta\phi'(\eta) - \phi(\eta)f'(\eta) + Sr\theta''(\eta) \right] = 0 \quad (2.10)$$

The corresponding boundary conditions are

$$\begin{aligned} f = fw, f' = \theta = \phi = 1 & \quad \text{at} & \quad y = 0 \\ f' = \theta = \phi = 0 & \quad \text{as} & \quad y \rightarrow \infty \end{aligned} \quad (2.11)$$

where the prime symbol represents the derivative with respect to  $\eta$  and  $fw$  is the suction parameter.

From the numerical computation, the local skin-friction coefficient, the local Nusselt number and Sherwood number which are respectively proportional to  $f''(0)$ ,  $-\theta'(0)$  and  $-\phi'(0)$  are worked out and their numerical values are presented in a tabular form.

### III. SOLUTION OF THE PROBLEM

The set of coupled non-linear governing boundary layer equations (2.8) - (2.10) together with the boundary conditions (2.11) are solved numerically by using Runge-Kutta fourth order technique along with shooting method. First of all, higher order non-linear differential Equations (2.8) - (2.10) are converted into simultaneous linear differential equations of first order and they are further transformed into initial value problem by applying the shooting technique (Jain *et al* [25]). The resultant initial value problem is solved by employing Runge-Kutta fourth order technique. The step size  $\Delta\eta=0.05$  is used to obtain the numerical solution. From the process of numerical computation, the skin-friction coefficient, the Nusselt number and the Sherwood number, which are respectively proportional to  $f''(0)$ ,  $-\theta'(0)$  and  $-\phi'(0)$ , are also sorted out and their numerical values are presented in a tabular form.

### IV. RESULTS AND DISCUSSION

The governing equations (2.9) - (2.11) subject to the boundary conditions (2.12) are integrated as described in section 3. Numerical results are reported in the Tables 1-2. The Prandtl number is taken to be  $Pr = 0.71$  which corresponds to air, the value of Schmidt number ( $Sc$ ) were chosen to be  $Sc = 0.24, 0.62, 0.78, 2.62$ , representing diffusing chemical species of most common interest in air like  $H_2$ ,  $H_2O$ ,  $NH_3$  and Propyl Benzene respectively.

The effects of various parameters on velocity profiles in the boundary layer are depicted in Figs. 1-10. In Fig. 1 the effect of increasing the magnetic field strength on the momentum boundary layer thickness is illustrated. It is now a well established fact that the magnetic field presents a damping effect on the velocity field by creating drag force that opposes the fluid motion, causing the velocity to decrease. Similar trend of slight decrease in the fluid velocity near the vertical plate is observed with an increase in suction parameter  $fw$  (see in Fig.2). Fig.3 illustrates the effect of the thermal Grashof number ( $Gr$ ) on the velocity field. The thermal Grashof number signifies the relative effect of the thermal buoyancy force to the viscous hydrodynamic force. The flow is accelerated due to the enhancement in buoyancy force corresponding to an increase in the thermal Grashof number, i.e. free convection effects. It is noticed that the thermal Grashof number ( $Gr$ ) influence the velocity field almost in the boundary layer when compared to far away from the plate. It is seen that as the thermal Grashof number ( $Gr$ ) increases, the velocity field increases. The effect of mass (solutal) Grashof number ( $Gc$ ) on the velocity is illustrated in Fig.4. The mass (solutal) Grashof number ( $Gc$ ) defines the ratio of the species buoyancy force to the viscous hydrodynamic force. It is noticed that the velocity increases with increasing values of the solutal Grashof number.

Fig.5 illustrates the effect of the Schmidt number ( $Sc$ ) on the velocity. The Schmidt number ( $Sc$ ) embodies the ratio of the momentum diffusivity to the mass (species) diffusivity. It physically relates the relative thickness of the hydrodynamic boundary layer and mass-transfer (concentration) boundary layer. It is noticed that as Schmidt number ( $Sc$ ) increases the velocity field decreases. Similar trend of slight decrease in the fluid velocity near the vertical plate is observed with an increase in Prandtl number  $Pr$  (see in Fig.6). Fig. 7 shows the variation of the velocity boundary-layer with the heat generation/absorption parameter ( $Q$ ). It is noticed that the velocity boundary layer thickness increases with an increase in the generation/absorption parameter. Fig. 8 shows the variation of the velocity boundary-layer with the Dufour number ( $D_f$ ). It is observed that the velocity boundary layer thickness increases with an increase in the Dufour number. Fig. 9 shows the variation of the velocity boundary-layer with the Soret number ( $Sr$ ). It is found that the velocity boundary layer thickness increases with an increase in the Soret number. Fig. 10 shows the variation of the velocity boundary-layer with the Unsteadiness parameter ( $A$ ). It is found that the velocity boundary layer thickness increases with an increase in the Unsteadiness parameter.

As per the boundary conditions of the flow field under consideration, the fluid temperature attains its maximum value at the plate surface and decreases exponentially to the free stream zero value away from the plate. This is observed in Figs. 11-20. The effect of the magnetic parameter  $M$  on the temperature is illustrated in Fig.11. It is observed that as the magnetic parameter  $M$  increases, the temperature increases. Fig.12 illustrates the effect of the suction parameter ( $fw$ ) on the temperature. It is noticed that as suction parameter increases, the temperature decreases. From Figs. 13 and 14, it is observed that the thermal boundary layer thickness decreases with an increase in the thermal or Solutal Grashof numbers ( $Gr$  or



$Gc$ ). Fig. 15 illustrates the effect of Schmidt number ( $Sc$ ) on the temperature. It is noticed that as the Schmidt number ( $Sc$ ) increases, an increasing trend in the temperature field is noticed. Much of significant contribution of Schmidt number ( $Sc$ ) is noticed as we move far away from the plate.

Fig.16 illustrates the effect of the Prandtl number ( $Pr$ ) on the temperature. It is noticed that as the Prandtl number increases, the temperature decreases. Fig.17 illustrates the effect of the heat generation/absorption parameter ( $Q$ ) on the temperature. It is noticed that as the heat generation/absorption parameter increases, the temperature increases. Fig. 18 shows the variation of the thermal boundary-layer with the Dufour number ( $D_f$ ). It is noticed that the thermal boundary layer thickness increases with an increase in the Dufour number. Fig. 19 shows the variation of the thermal boundary-layer with the Soret number ( $Sr$ ). It is observed that the thermal boundary layer thickness decreases with an increase in the Soret number. The effect of Unsteadiness parameter ( $A$ ) on the temperature field is illustrated Fig.20. As the Unsteadiness parameter increases the thermal boundary layer is found to be increasing.

Figs. 21 - 28 depict chemical species concentration against span wise coordinate  $\eta$  for varying values of physical parameters in the boundary layer. The species concentration is highest at the plate surface and decrease to zero far away from the plate satisfying the boundary condition. The effect of magnetic parameter ( $M$ ) on the concentration field is illustrated in Fig.21. As the magnetic parameter increases the concentration is found to be increasing. The effect of suction parameter ( $f_w$ ) on the concentration field is illustrated Fig.22. As the suction parameter increases the concentration is found to be decreasing. However, as we move away from the boundary layer, the effect is not significant. The effect of buoyancy parameters ( $Gr$ ,  $Gc$ ) on the concentration field is illustrated Figs. 23 and 24. It is noticed that the concentration boundary layer thickness decreases with an increase in the thermal or Solutal Grashof numbers ( $Gr$  or  $Gc$ ). Fig. 25 illustrates the effect of Schmidt number ( $Sc$ ) on the concentration. It is noticed that as the Schmidt number increases, there is a decreasing trend in the concentration field.

The influence of the heat generation/absorption parameter ( $Q$ ) on the concentration field is shown in Fig.26. It is noticed that the concentration decreases monotonically with the increase of the heat generation/absorption parameter. Fig. 27 shows the variation of the concentration boundary-layer with the Dufour number ( $D_f$ ). It is observed that the concentration boundary layer thickness decreases with an increase in the Dufour number. Fig. 28 shows the variation of the concentration boundary-layer with the Soret number ( $Sr$ ). It is found that the concentration boundary layer thickness increases with an increase in the Soret number.

In order to benchmark our numerical results, the present results for the skin -friction, Nusselt number and Sherwood number in the absence of  $M$ ,  $A$ ,  $f_w$ ,  $Q$ ,  $D_f$ ,  $Sr$  and  $S$  are compared with those of Magyari and Keller [24] and Srinivasachary and Ram Reddy [23] and found them in excellent agreement as demonstrated in Table 1. From Table 2, it is observed that the local skin-friction coefficient, local heat and mass transfer rates at the plate

increases with an increase in the buoyancy forces. It was noticed that the local skin-friction coefficient, local heat and mass transfer rates at the plate decreases with an increase in the Magnetic parameter. As the Prandtl number increases, both the skin-friction and Sherwood number decrease, whereas the Nusselt number increases. It was found that the local heat and mass transfer rate at the plate increases, but Skin-friction coefficient decreases with an increase in the Schmidt number or suction parameter. It is observed that the local heat and mass transfer rate at the plate decreases, whereas Skin-friction coefficient increases with an increase in the Unsteadiness parameter. As the Dufour number or heat generation/absorption parameter increases, both the skin-friction and Sherwood number increase, whereas the Nusselt number decreases. The effect of the Soret number is to increase the Skin-friction and the Nusselt number, and to decrease the Sherwood number.

## V. CONCLUSIONS

The present chapter analyzes the combined effect of the free convective heat and mass transfer on the unsteady two-dimensional boundary layer flow over a stretching vertical plate by taking heat generation/absorption, and soret and dufour effects into account. The governing equations are approximated to a system of non-linear ordinary differential equations by similarity transformation. Numerical calculations are carried out for various values of the dimensionless parameters of the problem. A comparison with previously published work is performed and excellent agreement between the results is found. The results are presented graphically and the conclusion is drawn that the flow field and other quantities of physical interest are significantly influenced by these parameters. It is noticed that as the heat generation/absorption parameter increases, the velocity and temperature increases, where as concentration decreases. The results for the prescribed skin friction, local heat and mass transfer rates at the plate are presented and discussed. It is found that the local skin-friction coefficient, local heat and mass transfer rates at the plate increase with an increase in the buoyancy forces. As the heat generation/absorption parameter or dufour number increases, both the skin-friction and Sherwood number increase, whereas the Nusselt number decreases. It is observed that the local skin-friction coefficient and local mass transfer rates at the plate decrease but Nusselt number decreases with an increase in the Prandtl number. The effect of the Soret number is to increase the local heat and mass transfer rates, and to decrease the skin-friction.

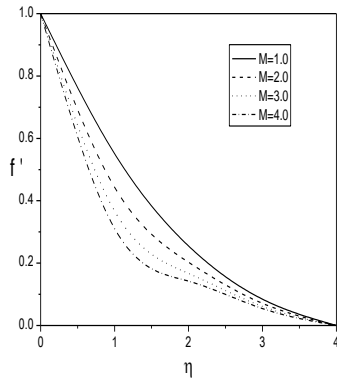


**Fig.1:** Variation of the velocity  $f'$  with  $M$  for  $Pr=0.71, Sc=0.24, Gr=Gc=A=1, Q=0.2, D_f=Sr=fw=0.1$ .

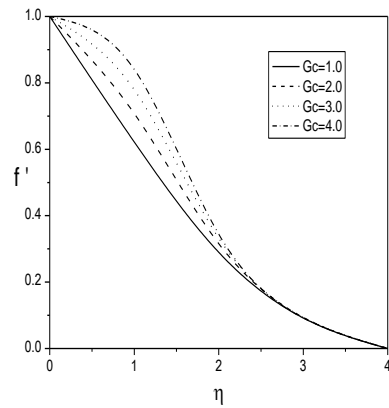


**Fig.4:** Variation of the velocity  $f'$  with  $Gc$  for  $Pr=0.71, Sc=0.24, Gr=A=1, Q=0.2, M=0.5, D_f=Sr=fw=0.1$ .

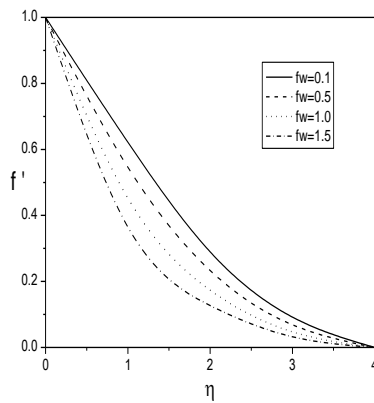


**Fig.2:** Variation of the velocity  $f'$  with  $fw$  for  $Pr=0.71, Sc=0.24, Gr=Gc=A=1, M=0.5, Q=0.2, D_f=Sr=0.1$ .

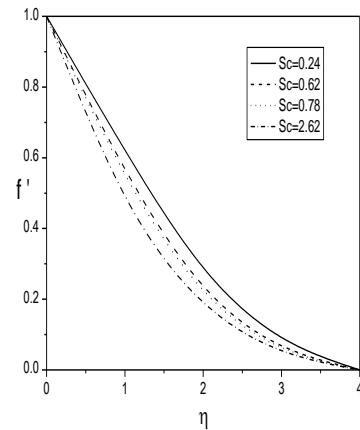


**Fig.5:** Variation of the velocity  $f'$  with  $Sc$  for  $Pr=0.71, Gr=Gc=A=1, Q=0.2, M=0.5, D_f=Sr=fw=0.1$ .

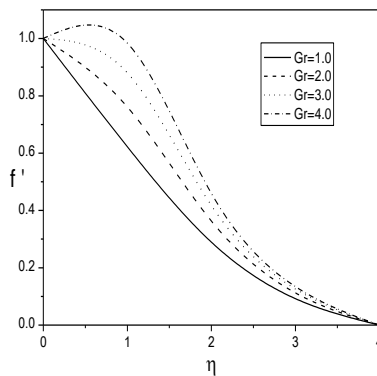


**Fig.3:** Variation of the velocity  $f'$  with  $Gr$  for  $Pr=0.71, Sc=0.24, Gc=A=1, M=0.5, Q=0.2, D_f=Sr=fw=0.1$ .

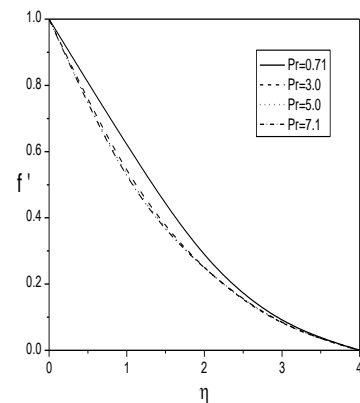


**Fig.6:** Variation of the velocity  $f'$  with  $Pr$  for  $Sc=0.24, Gr=Gc=A=1, Q=0.2, M=0.5, D_f=Sr=fw=0.1$ .

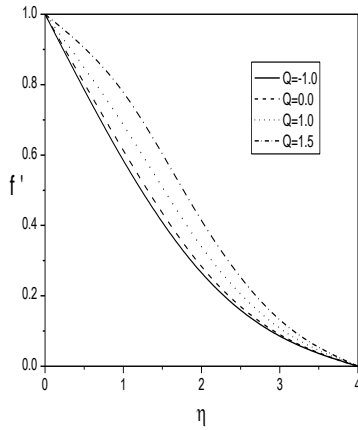


**Fig.7: Variation of the velocity  $f'$  with  $Q$  for  $Sc=0.24, Pr=0.71, Gr=Gc=A=1, M=0.5, D_f=Sr=fw=0.1$ .**

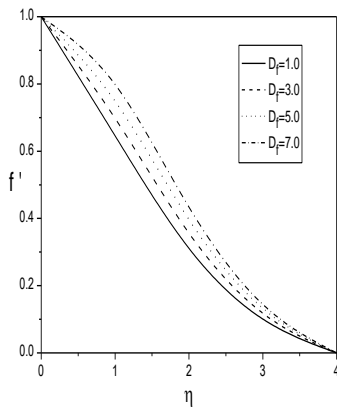


**Fig.8: Variation of the velocity  $f'$  with  $D_f$  for  $Pr=0.71, Sc=0.24, Gr=Gc=A=1, M=0.5, Q=0.2, Sr=fw=0.1$ .**

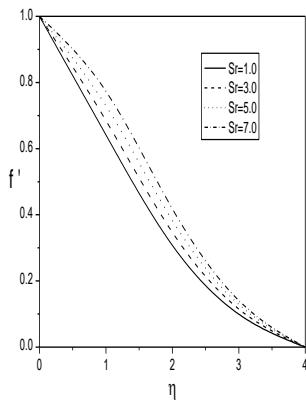


**Fig.9: Variation of the velocity  $f'$  with  $Sr$  for  $Pr=0.71, Sc=0.24, Gr=Gc=A=1, M=0.5, Q=0.2, D_f=fw=0.1$ .**

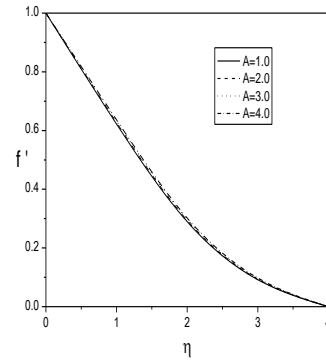


**Fig.10: Variation of the velocity  $f'$  with  $Sr$  for  $Pr=0.71, Sc=0.24, Gr=Gc=A=1, M=0.5, Q=0.2, D_f=fw=0.1$ .**

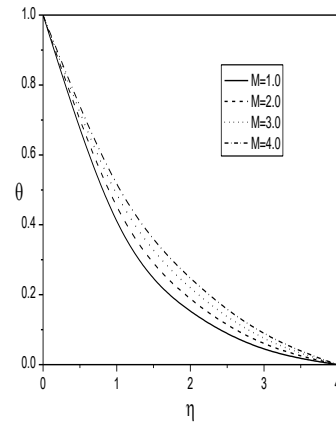


**Fig.11: Variation of the temperature  $\theta$  with  $M$  for  $Pr=0.71, Sc=0.24, Gr=Gc=A=1, Q=0.2, D_f=Sr=fw=0.1$ .**

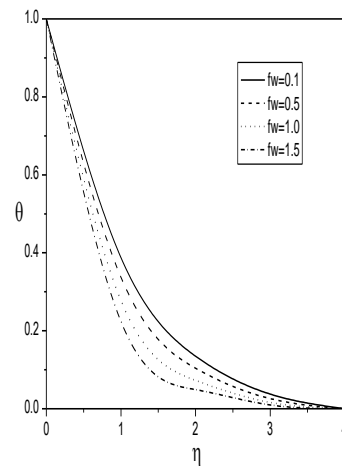


**Fig.12: Variation of the temperature  $\theta$  with  $fw$  for  $Pr=0.71, Sc=0.24, Gr=Gc=A=1, M=0.5, Q=0.2, D_f=Sr=0.1$ .**

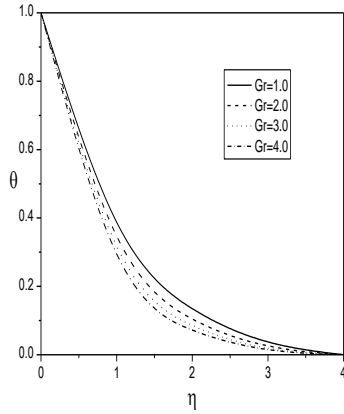


**Fig.13:** Variation of the temperature  $\theta$  with  $Gr$  for  $Pr=0.71$ ,  $Sc=0.24$ ,  $Gc=A=1$ ,  $M=0.5$ ,  $Q=0.2$ ,  $D_f=Sr=fw=0.1$ .

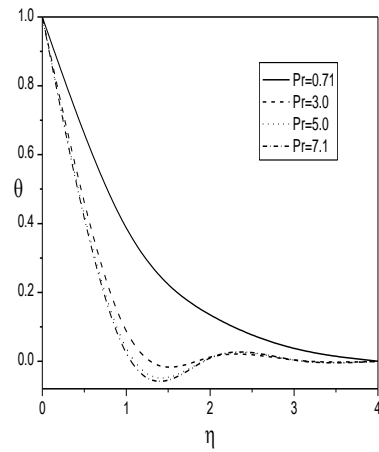


**Fig.16:** Variation of the temperature  $\theta$  with  $Pr$  for  $Sc=0.24$ ,  $Gr=Gc=A=1$ ,  $M=0.5$ ,  $Q=0.2$ ,  $D_f=Sr=fw=0.1$ .

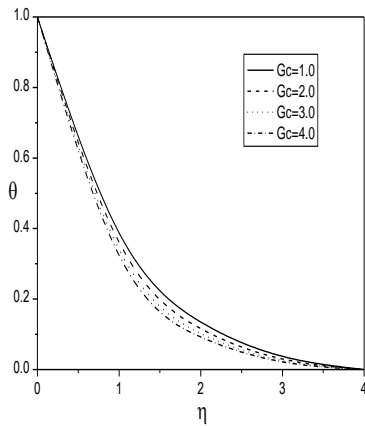


**Fig.14:** Variation of the temperature  $\theta$  with  $Gc$  for  $Pr=0.71$ ,  $Sc=0.24$ ,  $Gr=A=1$ ,  $M=0.5$ ,  $Q=0.2$ ,  $D_f=Sr=fw=0.1$ .

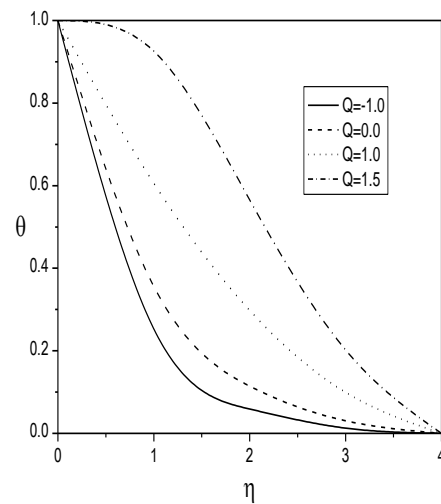


**Fig.17:** Variation of the temperature  $\theta$  with  $Q$  for  $Pr=0.71$ ,  $Sc=0.24$ ,  $Gr=Gc=A=1$ ,  $M=0.5$ ,  $D_f=Sr=fw=0.1$ .

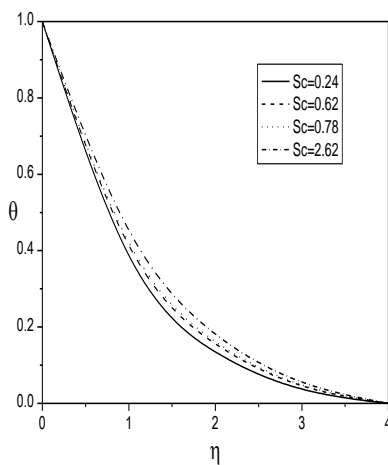


**Fig.15:** Variation of the temperature  $\theta$  with  $Sc$  for  $Pr=0.71$ ,  $Gr=Gc=A=1$ ,  $M=0.5$ ,  $Q=0.2$ ,  $D_f=Sr=fw=0.1$ .

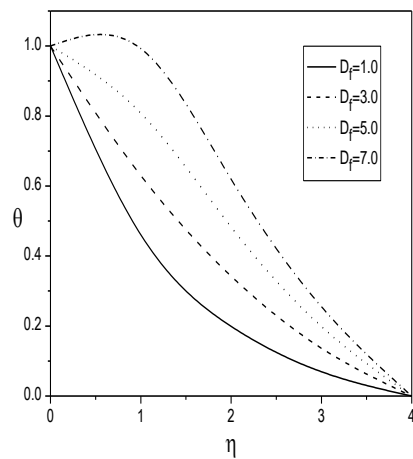


**Fig.18:** Variation of the temperature  $\theta$  with  $D_f$  for  $Pr=0.71$ ,  $Sc=0.24$ ,  $Gr=Gc=A=1$ ,  $M=0.5$ ,  $Q=0.2$ ,  $Sr=fw=0.1$ .

for  $Pr=0.71$ ,  $Sc=0.24$ ,  $Gr=Gc=A=1$ ,  $Q=0.2$ ,  
 $D_f=Sr=fw=0.1$ .

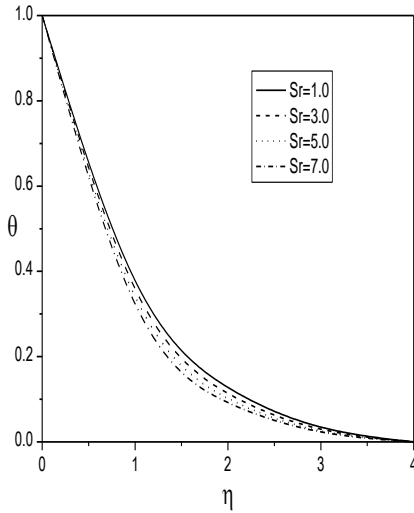


**Fig.19:** Variation of the temperature  $\theta$  with  $Sr$  for  $Pr=0.71$ ,  $Sc=0.24$ ,  $Gr=Gc=A=1$ ,  $M=0.5$ ,  $Q=0.2$ ,  $D_f=fw=0.1$ .

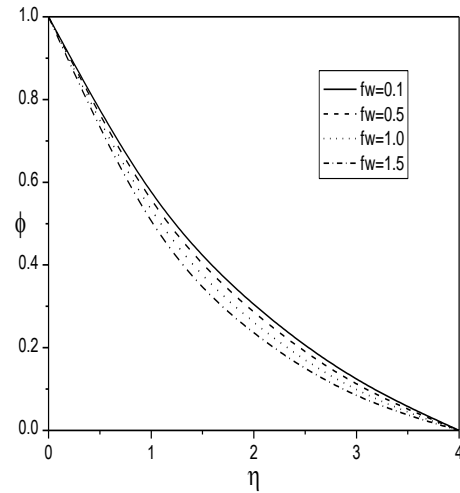


**Fig.22:** Variation of the concentration  $\phi$  with  $fw$  for  $Pr=0.71$ ,  $Sc=0.24$ ,  $Gr=Gc=A=1$ ,  $M=0.5$ ,  $Q=0.2$ ,  $D_f=Sr=0.1$ .

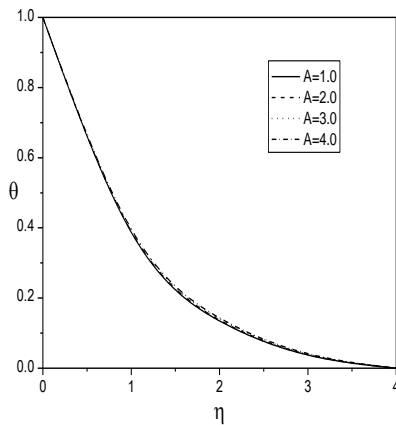


**Fig.20:** Variation of the temperature  $\theta$  with  $A$  for  $Pr=0.71$ ,  $Sc=0.24$ ,  $Gr=Gc=1$ ,  $M=0.5$ ,  $Q=0.2$ ,  $D_f=Sr=fw=0.1$ .

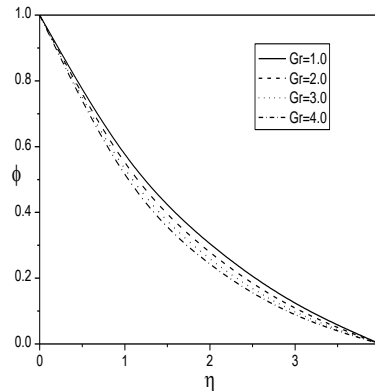


**Fig.23:** Variation of the concentration  $\phi$  with  $Gr$  for  $Pr=0.71$ ,  $Sc=0.24$ ,  $Gc=A=1$ ,  $M=0.5$ ,  $Q=0.2$ ,  $D_f=Sr=fw=0.1$ .

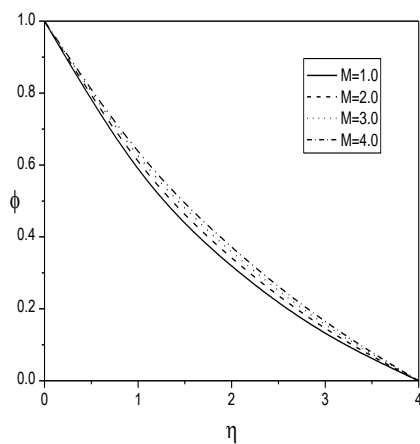


**Fig.21:** Variation of the concentration  $\phi$  with  $M$

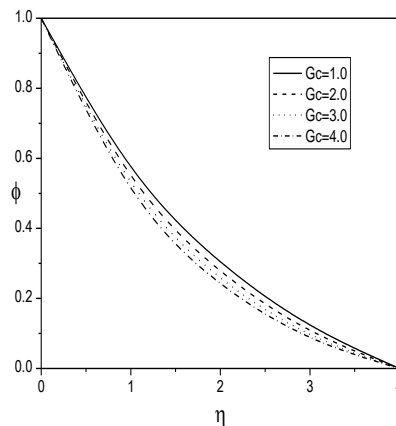


**Fig.24:** Variation of the concentration  $\phi$  with  $Gc$  for  $Pr=0.71$ ,  $Sc=0.24$ ,  $Gr=A=1$ ,  $M=0.5$ ,  $Q=0.2$ ,  $D_f=Sr=fw=0.1$ .



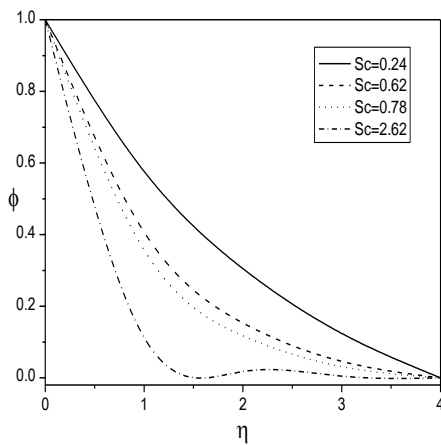


**Fig.25: Variation of the concentration  $\phi$  with  $Sc$  for  $Pr=0.71$ ,  $Gr=Gc=A=1$ ,  $M=0.5$ ,  $Q=0.2$ ,  $D_f=Sr=fw=0.1$ .**

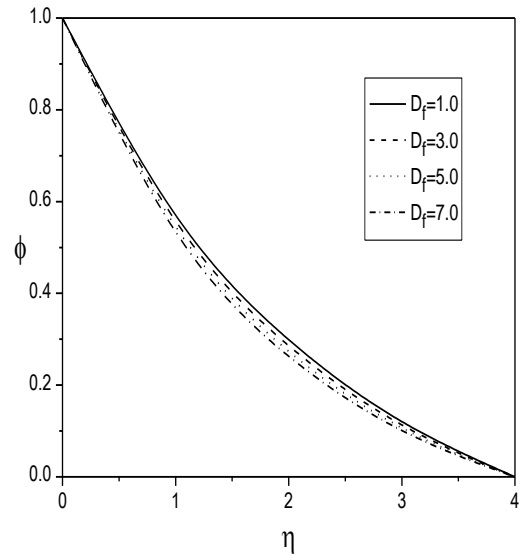


**Fig.27: Variation of the concentration  $\phi$  with  $D_f$  for  $Pr=0.71$ ,  $Sc=0.24$ ,  $Gr=Gc=A=1$ ,  $M=0.5$ ,  $Q=0.2$ ,  $Sr=fw=0.1$ .**

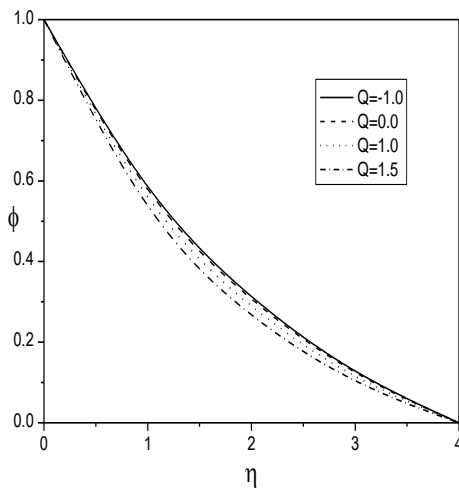


**Fig.26: Variation of the concentration  $\phi$  with  $Q$  for  $Pr=0.71$ ,  $Sc=0.24$ ,  $Gr=Gc=A=1$ ,  $M=0.5$ ,  $D_f=Sr=fw=0.1$ .**

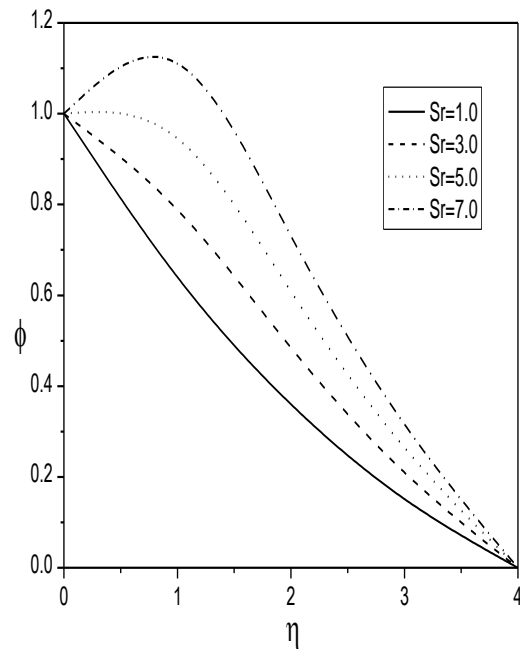


**Fig.28: Variation of the concentration  $\phi$  with  $Sr$  for  $Pr=0.71$ ,  $Sc=0.24$ ,  $Gr=Gc=A=1$ ,  $M=0.5$ ,  $Q=0.2$ ,  $D_f=fw=0.1$ .**

**able 1** Numerical values of  $\theta'(0)$  for  $Gr=Gc=Sr=D_f=Q=fw=0$  and  $Sc \rightarrow 0$ . Comparison of the present results with that of Magyari and keller [24], and Srinivasachary and Ram Reddy [23].

Pr	Magyari and keller [24]	Srinivasachary and Ram Reddy [23]	Present Results
0.5	-0.59434	-0.59438	-0.667192
1.0	-0.95478	-0.95478	-1.00426
3.0	-1.86908	-1.86908	-1.92168
5.0	-2.50014	-2.50015	-2.55594

8.0	-3.24213	-3.24218	-3.30016
10.0	-3.66038	-3.66043	-3.71928

**Table 2** Variation of  $f''(0)$ ,  $-\theta'(0)$  and  $-\phi'(0)$  at the plate with  $Gr$ ,  $Gc$ ,  $M$ ,  $Pr$ ,  $Sc$ ,  $Sr$ ,  $D_f$ ,  $A$ ,  $Q$ ,  $fw$ .

$Gr$	$Gc$	$M$	$Pr$	$Sc$	$Sr$	$D_f$	$A$	$Q$	$fw$	$f''(0)$	$-\theta'(0)$	$-\phi'(0)$
1	1	0.5	0.71	0.24	0.01	0.01	1	0.02	0.01	-0.268957	0.882380	0.527214
2	1	0.5	0.71	0.24	0.01	0.01	1	0.02	0.01	0.193829	0.949762	0.560834
1	2	0.5	0.71	0.24	0.01	0.01	1	0.02	0.01	0.115906	1.002640	0.588621
1	3	0.5	0.71	0.24	0.01	0.01	1	0.02	0.01	0.478782	0.949018	0.549084
1	1	5	0.71	0.24	0.01	0.01	1	0.02	0.01	-0.504938	0.967315	0.567495
1	1	1	0.71	0.24	0.01	0.01	1	0.02	0.01	-1.243580	0.844139	0.509469
1	1	0	1.01	0.24	0.01	0.01	1	0.02	0.01	-0.418908	0.723913	0.459550
1	1	1	0.71	0.24	0.01	0.01	1	0.02	0.01	-0.342720	2.013790	0.483456
1	1	3	0.71	0.24	0.01	0.01	1	0.02	0.01	-0.364602	2.706920	0.464043
1	1	5	3.04	0.24	0.01	0.01	1	0.02	0.01	-1.179407	0.387119	0.856410
1	1	0.5	5.01	0.24	0.01	0.01	1	0.02	0.01	-0.114296	0.822721	0.972591
1	1	0.5	0.71	0.62	0.01	0.01	1	0.02	0.01	-0.160599	0.933253	0.114921
1	1	0.5	0.71	0.24	3.01	0.01	1	0.02	0.01	-0.241963	0.968535	-0.200696
1	1	0.5	0.71	0.24	0.01	3.01	1	0.02	0.01	-0.428342	0.406943	0.555048
1	1	0.5	0.71	0.24	0.01	0.01	5.01	0.02	0.01	-0.684334	0.046733	0.574042
1	1	0.5	0.71	0.24	0.01	0.01	0.01	0.02	0.01	0.877468	0.872552	0.525047
1	1	0.5	0.71	0.24	0.01	0.01	0.01	0.02	0.01	0.872552	0.7392	0.522894

		5	0.7 1	4	1	1		5	1		13	0.53437 2
		0.		0.2	0.	0.		1.	0.		0.4188	
		5	0.7 1	4	1	1		0	1		66	0.55196 4
		0.		0.2	0.	0.		0.	0.		1.0279	
		5	0.7 1	4	1	1		2	5		40	0.56210 6
		0.		0.2	0.	0.		0.	1.		1.2347	
		5		4	1	1		2	0		70	0.60945 1

## REFERENCES

- Anderson, H.T., Aarseth, J.B. and Dandapat, B.S. (2000), Heat trans-fer in a liquid film on an unsteady stretching surface, *Int. J. Heat Transf.* Vol. 43, pp. 69-74.
- Ishak, A., Nazar, R., and Pop, I., (2007), "Magneto-hydrodynamic Stagnation Point Flow. Towards a Stretching Vertical Sheet in a Micropolar Fluid", *Magneto-hydrodynamics*, Vol. 43, pp. 83 – 97.
- Ishak, A., Nazar, R., and Pop, I. (2006), "Unsteady Mixed Convection Boundary Layer Flow Due to a Stretching Vertical Surface", *the Arabian Journal for Science and Engineering*, Vol. 31, pp. 165 – 182.
- Rajesh, V. (2010), MHD effects on free convection and mass transform flow through a porous medium with variable temperature, *Int. J. of Appl. Math and Mech.*, Vol. 6, No. 14, pp.1 – 16.
- El-Arabawy, H. A. M. (2003), Effect of Suction/Injection on a Micropolar Fluid Past a Continuously Moving Plate in the Presence of Radiation, *Int. J. Heat Mass Trans.*, vol.46, pp.1471-1477.
- Loganathan, P. (2010), Effects of Thermal Conductivity on Unsteady Mhd Free Convective Flow Over A Semi Infinite Vertical Plate, *International Journal of Engineering Science and Technology*, Vol. 2, No. 11, pp. 6257-6268.
- Kinyanjui, M., Wanza, J. K. K., and Uppal, S. M. (2001), Magneto-hydrodynamic free convection heat and mass transfer of a heat generating fluid past an impulsively started infinite vertical porous plate with Hall current and radiation absorption, *Energy Conversion and Management*, Vol. 42, No. 2, pp. 917–931.
- Al-Odat, M. Q. and Al-Azab, T. A. (2007), Influence of chemical reaction on transient MHD free convection over a moving vertical plate, *Emirates Journal for Engineering Research*, Vol. 12, No. 3, pp. 15–21.
- Palani, G. and Srikanth, U. (2009), MHD flow past a semi-infinite vertical plate with mass transfer. *Nonlinear Analysis, Modelling and Control*, Vol. 14, No. 3, pp. 345–356.
- Makinde, O. D. (2010), On MHD heat and mass transfer over a moving vertical plate with a convective surface boundary condition, *The Canadian Journal of Chemical Engineering*, Vol. 88, No. 6, pp. 983–990.
- Tania S. Khaleque and Samad M.A. (2010), Effects of radiation, heat generation and viscous dissipation on MHD free convection flow along a stretching sheet, *Research J of Appl. Sci., Eng. and Tech.*, Vol. 2, No. 4, pp. 368-377.
- Moalem .D. (1976), Steady state heat transfer with porous medium with temperature dependent heat generation, *Int. J.Heat and Mass Transfer*, Vol. 19, No. 529–537.
- Vajrevelu. K., J. Nayfeh, (1992), Hydro magnetic convection at a cone and a wedge, *Int. Comm. Heat Mass Transfer*, Vol. 19, pp. 701–710.
- Chamkha A. J. (1999), Hydro magnetic three-dimensional free convection on a vertical stretching surface with heat generation or absorption, *Int. J. Heat and Fluid Flow*, Vol. 20, pp. 84–92.
- Shankar, B., Prabhakar Reddy, B. And Ananda Rao, J. (2010), Radiation and mass transfer effects on MHD free convection fluid flow embedded in a porous medium with heat generation/absorption, *Indian Journal of pure and applied physics*, Vol. 48, pp.157-165.
- Eckert, E. R. G. and Drak, R. M. (1972), *Analysis of Heat and Mass Transfer*, McGraw-Hill, New York.
- Kafoussias, N. G. and Williams, E. W. (1995), Thermal-diffusion and diffusion-thermo effects on mixed free-forced convective and mass transfer boundary layer flow with temperature dependent viscosity. *International Journal of Engineering Science*, Vol. 33, No. 9, pp. 1369–1384.
- Mohamad, R. A. (2009), Double-diffusive convection-radiation interaction on unsteady MHD flow over a vertical moving porous plate with heat generation and Soret effect, *Applied Mathematical Sciences*, Vol. 3, No. 13, pp. 629–651.
- Afify, A. A. (2009), Similarity solution in MHD: effects of thermal-diffusion and diffusion-thermo on free convective heat and mass transfer over a stretching surface considering suction or injection, *Communications in Nonlinear Science and Numerical Simulation*, Vol. 14, No. 5, pp. 2202–2214.
- Shyam, S. T., Rajeev, M., Rohit, K. G., and Aiyub, K. (2010), MHD free convection-radiation interaction along a vertical surface embedded in Darcian porous medium in presence of Soret and Dufour's effects, *Thermal Science*, Vol. 14, No. 1, pp.137–145.
- Al-Odat, M.Q. and Al-Ghamdi, A. (2012), Dufour and Soret effects on unsteady MHD natural convection flow past vertical plate embedded in non-Darcy porous medium, *Appl. Math. Mech. -Engl. Ed.*, Vol.33, No.2, pp.195–210.
- Ali-Chamkha, M. A. and Mansour, A. A. (2011), Unsteady MHD free convective heat and mass transfer from a vertical porous plate with Hall current, thermal radiation and chemical reaction effects, *International Journal for Numerical Methods in Fluids*, Vol.65, No.4, pp.432–447.
- Srinivasacharya, D. and RamReddy, Ch. (2011), Soret and Dufour Effects on Mixed Convection from an Exponentially Stretching Surface, *International Journal of Nonlinear Science*, Vol.12, No.1, pp.60-68.
- Magyari, E. and Keller, B (1999), Heat and mass transfer in the boundary layers on an exponentially stretching continuous surface, *J. Phys. D: Appl. Phys.*, Vol.32, and No.577-585.
- Jain, M.K., Iyengar, S.R.K., and Jain, R.K. (1985), *Numerical Methods for Scientific and Engineering Computation*, Wiley Eastern Ltd., New Delhi, India.